This is an open access article published under an ACS AuthorChoice License, which permits copying and redistribution of the article or any adaptations for non-commercial purposes.

molecular pharmaceutics

Article

pubs.acs.org/molecularpharmaceutics

^{44}Sc: An Attractive Isotope for Peptide-Based PET Imaging

Reinier Hernandez,[†] Hector F. Valdovinos,[†] Yunan Yang,[‡] Rubel Chakravarty,[‡,§] Hao Hong,[‡] Todd E. Barnhart,[†] and Weibo Cai*[,†,‡,∥]

[†]Department of Medical Physics, University of Wisconsin−Madison, Madison, Wisconsin 53706, United States

[‡]Department of Radiology, University of Wisconsin−Madison, Madison, Wisconsin 53706, United States

[§]Isotope Production and Applications Division, Bhabha Atomic Research Centre, Mumbai 400085, India

[∥]University of Wisconsin Carbone Cancer Center, Madison, Wisconsin 53792, United States

Supporting Information

ABSTRACT: The overexpression of integrin $\alpha_v\beta_3$ has been linked to tumor aggressiveness and metastasis in several cancer types. Because of its high affinity, peptides containing the arginine−glycine−aspartic acid (RGD) motif have been proven valuable vectors for noninvasive imaging of integrin $\alpha_v\beta_3$ expression and for targeted radionuclide therapy. In this study, we aim to develop a ^{44}Sc-labeled RGD-based peptide for *in vivo* positron emission tomography (PET) imaging of integrin $\alpha_v\beta_3$ expression in a preclinical cancer model. High quality ^{44}Sc ($t_{1/2}$, 3.97 h; β^+ branching ratio, 94.3%) was produced inexpensively in a cyclotron, via proton irradiation of natural Ca metal targets, and separated by extraction chromatography. A dimeric cyclic-RGD peptide, $(cRGD)_2$, was conjugated to 1,4,7,10-tetraazacyclododecane-1,4,7,10-tetraacetic acid (DOTA) and radiolabeled with ^{44}Sc in high yield (>90%) and specific activity (7.4 MBq/nmol). Serial PET imaging of mice bearing U87MG tumor xenografts showed elevated ^{44}Sc-DOTA-$(cRGD)_2$ uptake in the tumor tissue of 3.93 ± 1.19, 3.07 ± 1.17, and 3.00 ± 1.25 %ID/g at 0.5, 2, and 4 h postinjection, respectively (n = 3), which were validated by *ex vivo* biodistribution experiments. The integrin $\alpha_v\beta_3$ specificity of the tracer was corroborated, both *in vitro* and *in vivo*, by competitive cell binding and receptor blocking assays. These results parallel previously reported studies showing similar tumor targeting and pharmacokinetic profiles for dimeric cRGD peptides labeled with ^{64}Cu or ^{68}Ga. Our findings, together with the advantageous radionuclidic properties of ^{44}Sc, capitalize on the relevance of this isotope as an attractive alternative isotope to more established radiometals for small molecule-based PET imaging, and as imaging surrogate of ^{47}Sc in theranostic applications.

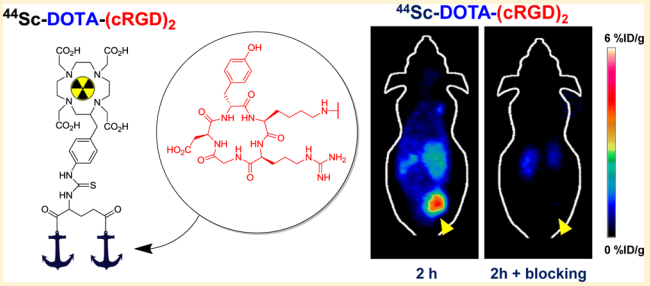

KEYWORDS: *scandium-44 (^{44}Sc), arginine−glycine−aspartic acid (RGD) peptides, RGD dimer, integrin $\alpha_v\beta_3$, tumor angiogenesis, positron emission tomography (PET), molecular imaging*

INTRODUCTION

Angiogenesis, new blood vessel formation, is the process by which tumors circumvent oxygen and nutrient limitations and acquire an aggressive character.[1−3] Abnormal angiogenesis is recognized as an indispensable process in tumor progression and metastasis.[4] The regulation of angiogenesis is governed by a delicate balance between a myriad of pro-angiogenic and antiangiogenic factors.[5] Among those, integrins play a substantial role in inducing and maintaining neovasculature proliferation.[6] Within this family, integrin $\alpha_v\beta_3$ has been found overexpressed primarily in activated endothelial cells and on the surface of many tumor cells including high grade glioma, breast cancer, ovarian cancer, and melanoma.[7−9] Given that in many cancer types there is a positive correlation between the differential expression of integrin $\alpha_v\beta_3$ and histological grade, the targeting of this membrane protein for diagnostic and therapy purposes have been extensively pursued.[10] In fact, treatment with antagonists of integrin $\alpha_v\beta_3$ has demonstrated inhibition of tumor angiogenesis and metastasis.[11−13] Thus, noninvasive imaging of the integrin $\alpha_v\beta_3$ expression is of paramount importance to identify patient populations that might benefit from antiangiogenic therapy and to monitor the efficacy of such approaches.[6,14,15]

Integrin $\alpha_v\beta_3$ is a cell adhesion molecule that clings to the arginine−glycine−aspartic acid (RGD) sequences present in extracellular matrix proteins such as fibrinogen, fibronectin, and vitronectin.[11,16] Containing the same RGD motif, a plethora of peptide-based tracers has been developed to target integrin $\alpha_v\beta_3$ in several malignancies.[17,18] In particular, cyclic RGD peptides have been extensively evaluated as radiotracers for positron emission tomography (PET) and single photon emission

Received: May 7, 2014
Revised: June 23, 2014
Accepted: July 15, 2014
Published: July 15, 2014

 © 2014 American Chemical Society

computed tomography (SPECT) imaging of integrin $\alpha_v\beta_3$-positive tumors. The first integrin $\alpha_v\beta_3$-specific PET tracer was developed over a decade ago and featured a ^{18}F-labeled glycosylated pentapeptide, [^{18}F]Galacto-RGD.[19,20] Subsequently, several other fluorinated tracers have been reported, many of which showing positive results for the noninvasive visualization of integrin $\alpha_v\beta_3$ expression in humans.[21,22] Nevertheless, the clinical implementation of these ^{18}F-based tracers has been hampered by several practical problems such as their relatively low tumor uptake, cumbersome radiosynthesis, and the requirement of a nearby cyclotron facility.

A different family of radiotracers based on radiometals has emerged that addresses some of the challenges plaguing ^{18}F-based agents. Two radionuclides with favorable properties, ^{68}Ga ($t_{1/2}$ = 68 min, E_{mean} (β^+) = 830 keV, branching ratio = 89%) and ^{64}Cu ($t_{1/2}$ = 12.7 h, E_{mean} (β^+) = 278 keV, branching ratio = 17.6%), have dominated the application of positron-emitting metals for radiolabeling of small-molecule agents. The availability of commercial ^{68}Ge/^{68}Ga generators and its facile radiolabeling using peptides conjugated to macrocyclic ligands make ^{68}Ga an attractive choice for clinical applications.[23] However, the short decay half-life of ^{68}Ga restricts its use to in-house labeling of small molecules. Furthermore, the relatively high cost of the generators and perhaps more importantly the requirement for extensive postelution purification and concentration of ^{68}Ga to eluate due to ^{68}Ge and sorbent material breakthrough render this isotope of limited utility in a clinical setting.[24] However, the longer half-life of ^{64}Cu allows for more flexible radiochemistry, and for its centralized production and posterior distribution to nuclear medicine facilities without a cyclotron.[25] Nevertheless, ^{64}Cu presents relatively low positron branching ratio (17.6%) and concomitant emission of β^- particles, which significantly increases the radiation doses imparted by this radionuclide.

The use of ^{44}Sc ($t_{1/2}$ = 3.97 h, E_{mean} (β+) = 632 keV, branching ratio = 94.3%) may offer several advantages. With a high positron fraction and nearly four times the half-life of ^{68}Ga, ^{44}Sc facilitates the synthesis of a wider variety of radiotracers with longer pharmacokinetic profiles while giving enough room for its posterior transportation to distant PET facilities. Additionally, the existence of ^{47}Sc, an isotope with tremendous potential for radionuclide therapy, creates the opportunity for seamless employment of ^{44}Sc/^{47}Sc isotopic pair in disease diagnosis, dosimetry estimation, therapy, and assessment of therapeutic responses.[26,27]

Currently there are two main routes for ^{44}Sc production: ^{44}Ti/^{44}Sc generators and via cyclotron irradiation of ^{44}Ca targets through ^{44}Ca(p,n)^{44}Sc reaction. Although the development of a 5 mCi (185 MBq) ^{44}Ti/^{44}Sc generator has been reported,[28] due to difficulties in the production of the parent isotope (^{44}Ti), the applicability of this generator is very limited making its clinical implementation improbable. However, cyclotron production of ^{44}Sc has been proven feasible and cost-efficient by several research groups. For example, we recently demonstrated that ^{44}Sc can be produced inexpensively with adequate yields and radionuclidic purity by irradiating natural metallic Ca targets.[29]

To date, a limited number of studies have described the production and implementation of ^{44}Sc radiopharmaceutical for PET imaging, the majority of them showing only modest success *in vivo*.[27,30] To the best of our knowledge, herein we report the first instance of the development of a peptide-based radiotracer for PET imaging using cyclotron produced ^{44}Sc. Also, we demonstrated that ^{44}Sc obtained from the proton irradiation of unenriched Ca targets and separated via extraction chromatography resulted in a quality product with high radionuclide purity and specific activity, in a highly cost-efficient manner. We also accomplished the synthesis and ^{44}Sc-labeling of a dimeric cyclic RGD peptide, denoted as $(cRGD)_2$, using 1,4,7,10-tetraazacyclododecane-*N*,*N*′,*N*″,*N*‴-tetraacetic acid (DOTA) as the chelator. *In vivo* integrin $\alpha_v\beta_3$ targeting evaluation in a human glioblastoma animal model demonstrated that ^{44}Sc is a viable alternative to other radiometals (e.g., ^{68}Ga and ^{64}Cu) for peptide-based PET applications.

EXPERIMENTAL SECTION

Reagents. All purchased chemicals were of the highest purity available and used without further purification. Metallic natural Ca (99.999%) and Chelex 100 resin (50−100 mesh) were obtained from Sigma-Aldrich (St. Louis, MO). $(cRGD)_2$ was obtained from Peptide International Inc. (Louisville, KY) and 2-(*p*-isothiocyanatobenzyl)-1,4,7,10-tetraazacyclododecane-*N*,*N*′,*N*″,*N*‴-tetraacetic acid (*p*-SCN-Bn-DOTA) was purchased from Macrocyclics (Dallas, TX). Diamyl, amylphosphonate extraction resin (UTEVA) was acquired from Eichrom Technologies LLC (Lisle, IL). The rest of the materials and reagents were obtained from Thermo Fisher Scientific (Fair Law, NJ). Water and all buffers were of Milli-Q grade (resistivity > 18.2 MΩ·cm) and were treated with Chelex 100 resin to remove heavy metal contaminants.

^{44}Sc Production and Separation. Approximately 300 mg of natural Ca metal were pressed with a hydraulic press into an aluminum target holder and covered with a 25 μm thick molybdenum foil. One hour irradiations of the targets with 15.56 MeV proton were performed on the UW-Madison PETtrace cyclotron, with an average current of 25 μA and activity yield of 32 ± 3 MBq/μA·h (n = 10) at the end of bombardment (EoB). After irradiation, the calcium targets were removed from the holders and dissolved in 10 mL of concentrated HCl for a final H^+ concentration of ∼10.5 M. The target solution was then passed through a 0.5 cm diameter column packed with 50 mg of UTEVA extraction resin that was previously equilibrated with 0.5 mL of 10 M HCl. A wash step with 5 mL of 10 M HCl was performed to remove bulk Ca and other impurities. Approximately 80% of the ^{44}Sc activity produced at EoB was eluted with water in 2 × 200 μL fractions. In order to minimize radiation exposure, all separation steps were performed in a custom-made semi-automatic module. Gamma spectra were acquired with a high purity Ge (HPGe) detector (Canberra C1519) to determine ^{44}Sc radionuclidic purity.

DOTA Conjugation and Radiolabeling. DOTA-$(cRGD)_2$ conjugate was prepared as previously described.[31] Briefly, 2 mg (∼1.5 μmol) of $(cRGD)_2$ were dissolved in phosphate buffer saline (PBS) at a concentration of 5 mg/mL, and the pH was adjusted to 8.5−9.0 with 0.1 M Na_2CO_3. Two milligrams (∼3.0 μmol) of *p*-SCN-Bn-DOTA were dissolved in 50 μL of anhydrous dimethyl sulfoxide (DMSO) and immediately added to the $(cRGD)_2$ solution. The pH was readjusted to 8.5−9.0 with 0.1 M Na_2CO_3, and the reaction was allowed to proceed for 2 h at room temperature under gentle mixing. DOTA-$(cRGD)_2$ was isolated by semipreparative reverse phase HPLC (column, Phenomenex Luna C18, 5 μm, 10 × 250 mm; flow, 5 mL/min; mobile phase, 5−65% acetonitrile/water linear gradient in 40 min) and lyophilized to

dx.doi.org/10.1021/mp500343j | *Mol. Pharmaceutics* 2014, 11, 2954−2961

afford a white powder. Matrix-assisted laser desorption ionization (MALDI) time-of-flight mass spectrometry (TOF-MS) was performed to confirm DOTA-$(cRGD)_2$ identity ($[M + H]^+$: 1901.85).

Optimization of the radiolabeling conditions was performed by varying the reaction times and the ^{44}Sc/DOTA-$(cRGD)_2$ ratio. Three reaction vials were set containing 18.5 MBq of ^{44}Sc in 500 μL of 0.5 M NaOAc (pH = 4.5) and increasing concentrations (0.5, 1.3, and 2.6 nmol) of DOTA-$(cRGD)_2$. The solutions were incubated at 90 °C under constant agitation and samples of the reaction mixture taken at 5, 10, 15, 30, and 60 min. Reaction samples were spotted onto aluminum backed silica gel thin-layer liquid chromatography (TLC) plates (EMD Chemicals, Gibbstown, NJ). The plates were developed using 0.1 M sodium citrate (pH 4.5) as mobile phase for 15 min and dried. The ^{44}Sc-DOTA-$(cRGD)_2$ complex remained at the origin (R_f = 0.0−0.2), while the free radionuclide advanced with the solvent front (R_f = 0.6−1.0). The activity distribution on the plates was determined with a Packard Cyclone Phosphor-Plate imaging system (PerkinElmer).

^{44}Sc-DOTA-$(cRGD)_2$ for imaging studies was prepared using the optimized reaction conditions. First, 148 MBq (~100 μL) of ^{44}Sc activity were diluted in 1 mL of 0.5 M sodium acetate (pH 4.5), and 20 μL of a DOTA-$(cRGD)_2$ stock solution (1 mg/mL) were added. The reaction was then incubated at 90 °C for 15 min under constant agitation, and ^{44}Sc-DOTA-$(cRGD)_2$ was separated by radio-HPLC (column, Acclaim 120 C18, 5 μm, 4.6 × 250 mm; flow, 1 mL/min; mobile phase, 5−65% ethanol/water linear gradient in 40 min). The purified radioactive fraction was collected, diluted in PBS for a final <10% EtOH concentration, and filtered through a 20 μm syringe filter.

Cell Lines and Animal Models. U87MG human glioblastoma cells were purchased from the American Type Culture Collection (ATCC, Manassas, VA) and cultured in DMEM medium (Invitrogen, Carlsbad, CA) with 10% fetal bovine serum at 37 °C in a 5% CO_2 atmosphere. Cells were used for *in vitro* and *in vivo* experiments when they reached ~80% confluence. All animal studies were conducted under a protocol approved by the University of Wisconsin Institutional Animal Care and Use Committee. Female athymic nude mice (4−5 weeks old) were purchased from Harlan (Indianapolis, IN), and U87MG tumors were established by subcutaneous (s.c.) injection of 5 × 10^6 cells, suspended in 100 μL of 1:1 mixture of DMEM medium and Matrigel (BD Biosciences, Franklin lakes, NJ), into the lower right flank of the animal. Tumor size was visually monitored every other day, and *in vivo* experiments were performed when tumors reached 5−10 mm in diameter.

Competitive Cell Binding Assay. The *in vitro* binding affinities and specificities of $(cRGD)_2$ and DOTA-$(cRGD)_2$ for integrin $\alpha_v\beta_3$ were determined by a competitive binding assay with ^{125}I-Echistatin (PerkinElmer, Waltham, MA) as the integrin-specific radioligand. The assay was performed in U87MG human glioblastoma cells using a previously described method with slight modifications.[4] Briefly, 1 × 10^5 U87MG cells where seeded into 96-well filter plates (EMD Millipore Corp., Billerica, MA) and ^{125}I-Echistatin (~10,000 cpm) was added to the wells containing increasing concentration of the RGD-based peptides. Plates were incubated for 2 h at room temperature, and wells were washed with PBS to remove unbound activity. Finally, plates were dried, and the PVDF filters were removed and counted in an automated γ-counter (PerkinElmer, Waltham, MA). All samples were collected in triplicate, and binding curves were analyzed to determine the 50% inhibition concentration (IC_{50}) values using GraphPad Prism (GraphPad Software, San Diego, CA). All concentrations were expressed in a per molecule basis instead of a per cRGD moiety basis.

Small Animal PET Imaging. Mice bearing U87MG tumor xenografts were intravenously (i.v.) injected with 5.5−7.4 MBq of ^{44}Sc-DOTA-$(cRGD)_2$. Sequential PET scans were acquired at 0.5, 2, and 4 h after the injection of the tracer in an Inveon microPET/microCT scanner (Siemens Preclinical Solutions, Knoxville, TN). Mice were anesthetized by isoflurane inhalation and placed in a prone position in the scanner. In order to improve the detection statistics and minimize interscan variability due to radioactive decay, 20 million coincidence events per mouse were acquired for every static PET emission scan (energy window, 350−650 keV; time window, 3.432 ns; resolution, 1.5 mm). CT images were obtained prior to PET scans and used for anatomical coregistration with PET images and for attenuation correction purposes (80 kV, 900 μA, resolution 105 μm). To assess the *in vivo* integrin $\alpha_v\beta_3$ specificity, a receptor blocking experiment was carried out by coinjecting 3.7 MBq of ^{44}Sc-DOTA-$(cRGD)_2$ and 50 mg/kg (~1 mg) of $(cRGD)_2$.

Image reconstructions of PET scans were carried out on an Inveon Acquisition Workplace (Siemens Preclinical Solutions, Knoxville, TN) workstation using an ordered subset expectation maximization 3D/maximum *a posteriori* (OSEM3D/MAP) reconstruction algorithm. Region-of-interest (ROI) analysis of the PET images was performed using Inveon Research Workplace software (Siemens Preclinical Solutions, Knoxville, TN) and the tissue uptake values presented as percentage injected dose per gram (%ID/g).

Biodistribution Studies. *Ex vivo* biodistribution studies were perform to validate PET results and to obtain a more complete profile of the tissue distribution of the tracer. Immediately after the last PET scan at 4 h postinjection (p.i.), mice were euthanized by CO_2 asphyxiation, and blood, U87MG tumor, and all major organ/tissues were collected and weighted. The radioactivity of each tissue was counted in an automated γ-counter, and the tissue uptakes were calculated and reported as %ID/g (mean ± SD).

Statistical Analysis. Quantitative data were expressed as mean ± SD. Means were compared using two sample Student's *t* test; $p < 0.05$ was considered statistically significant.

RESULTS

^{44}Sc Production and Separation. Spectral analysis of the irradiated target revealed the predominance of ^{44}Sc over other coproduced radionuclidic impurities (Figure S1, Supporting Information), which was in agreement with previous data reported using the same production method.[29] Specifically, the activities corresponding to the major contaminants ^{43}Sc, ^{44m}Sc, ^{47}Sc, and ^{48}Sc were determined to account for less than 5% of the total activity generated at EoB; Table 1 shows a more detailed description of the impurities present on the product. The amount of activity and purities attained were more than satisfactory for our imaging applications; however, further optimization of the production parameter could improve the product, in cases where higher activities and/or radionuclidic purities were required.

The irradiated Ca pellets were easily dissolved in concentrated HCl and directly loaded into the UTEVA

Table 1. Description of the Major Radionuclidic Impurities Present on the Irradiated ^{nat}Ca Target

isotope	decay mode	$T_{1/2}$ (h)	measured impurities at EoB (%)[b]	calculated impurities 8 h after EoB (%)[c]
^{43}Sc	β^+ (88.1%)	3.89	2.57 ± 0.33	2.39
^{44m}Sc	IT (98.8%)[a]	58.6	0.57 ± 0.06	2.01
^{47}Sc	β^- (100%)	80.4	0.76 ± 0.08	2.59
^{48}Sc	β^- (100%)	43.7	0.38 ± 0.05	1.46
^{44}Sc purity			95.72%	91.56%

[a]IT: isomeric transition, typical of metastable isotopes. [b]Radionuclinic impurities at EoB are expressed as mean ± SD (n = 6). [c]Eight hour impurity levels were calculated from the initial mean values and using the exponential decay equation.

column. The strong Sc affinity of UTEVA at high HCl concentrations allowed the use of minimal amount of the resin material (50 mg), which facilitated the implementation of a compact automated separation system and minimized the amount of absorbed impurities in the column. The drastic reduction of Sc absorption coefficients at low HCl molarities[32] permitted the recovery of more than 80% of the initial (corrected to EoB) ^{44}Sc activity in 400 μL, for an average activity concentration of 925 MBq/mL and final concentration of ~1 M HCl. Overall, the separation was accomplished within 20 min after dissolution of the target, and the product was directly used for radiolabeling without the need for further purification/concentration steps.

Synthesis and Radiolabeling of DOTA-(cRGD)$_2$. DOTA-(cRGD)$_2$ (Figure 1A) was synthesized by direct conjugation of (cRGD)$_2$ with a 2-fold molar excess of *p*-SCN-Bn-DOTA under alkaline conditions (PBS, pH 9.0). Purification of DOTA-(cRGD)$_2$ was accomplished by reverse phase HPLC using a standard water/acetonitrile linear gradient, and the purified product was lyophilized. Figure 1B shows the MALDI-TOF mass spectrometry analysis of the sample, which corroborated the identity of the compound ($C_{83}H_{120}N_{24}O_{26}S$: m/z 1901.8 for $[M + H]^+$ vs 1900.85 calculated exact mass). Radiolabeling of DOTA-(cRGD)$_2$ with ^{44}Sc was performed under optimized conditions (Figure S3, Supporting Information) to attain radiochemical yields greater than 90% and specific activities higher than 7.1 MBq/nmol. A modified HPLC protocol that employed a water/ethanol linear gradient was used to purify ^{44}Sc-DOTA-(cRGD)$_2$, eliminating the need for the evaporation step required when nonbiocompatible solvent are used (e.g., acetonitrile).

Competitive Cell Binding Assay. We determined and compared the binding affinities of cRGD, (cRGD)$_2$, and DOTA-(cRGD)$_2$ for integrin $\alpha_v\beta_3$ in a competitive cell binding assay (Figure 2). A concentration-dependent displacement of the bound ^{125}I-Echistain was observed upon the addition of the RGD-based competitors. The IC_{50} values for cRGD, (cRGD)$_2$, and DOTA-(cRGD)$_2$ were 508 ± 87, 66 ± 10, and 316 ± 38 nM, respectively. The 10-fold higher affinity of (cRGD)$_2$

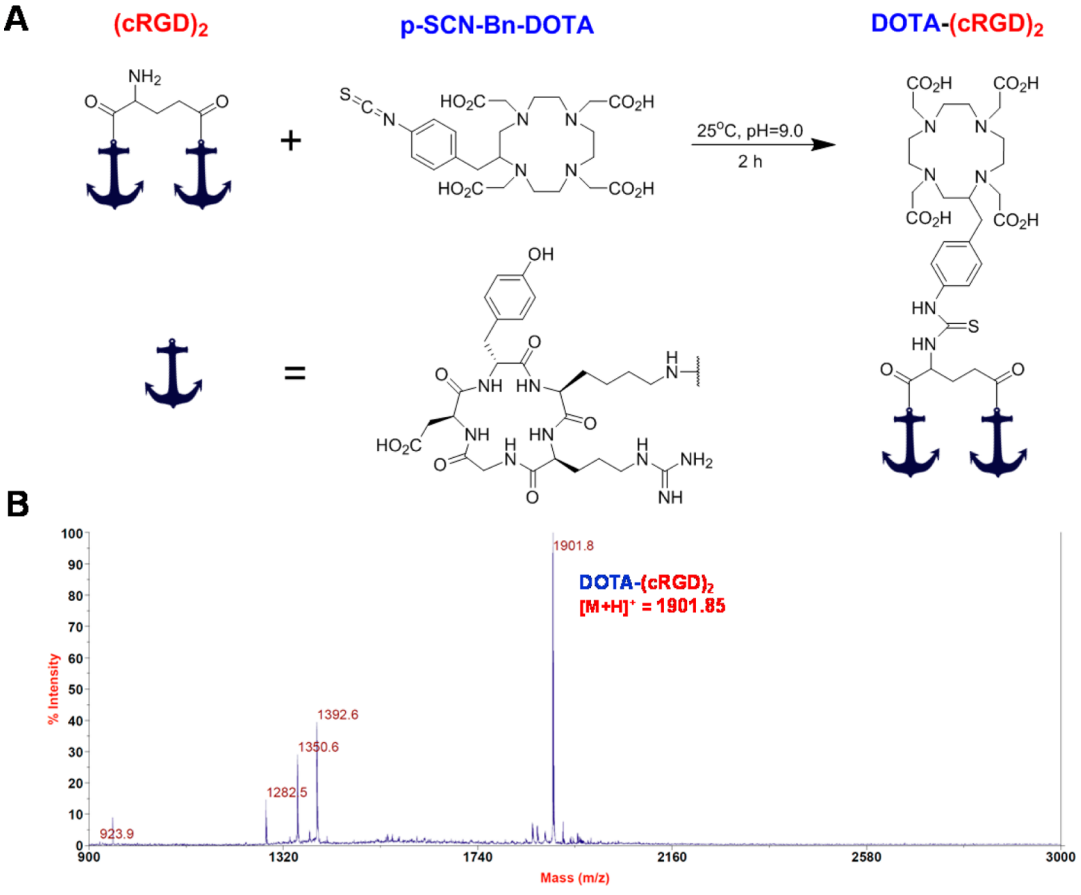

Figure 1. Schematic representation of the synthesis and characterization of DOTA-(cRGD)$_2$. (A) Bioconjugation of (cRGD)$_2$ with *p*-SCN-Bn-DOTA. (B) MALDI-TOF mass spectrum of DOTA-(cRGD)$_2$: exact $[M + H]^+$ = 1901.85; measured $[M + H]^+$ = 1901.8.

dx.doi.org/10.1021/mp500343j | *Mol. Pharmaceutics* 2014, 11, 2954−2961

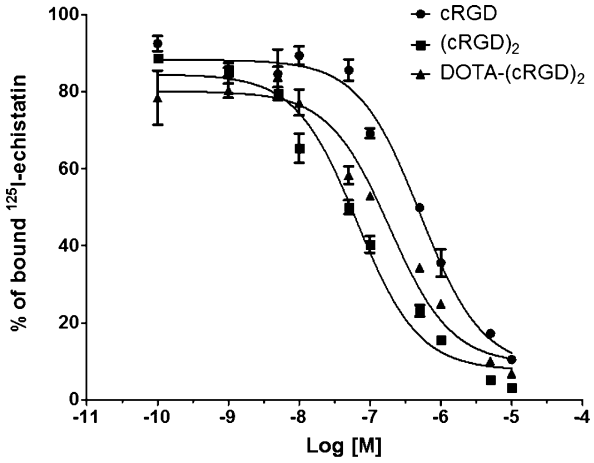

Figure 2. Inhibition of ^{125}I-echistatin binding to integrin $\alpha_v\beta_3$ on human glioblastoma (U87MG) cells by cRGD, $(cRGD)_2$, and DOTA-$(cRGD)_2$. Solid circles: cRGD (IC_{50} of 508 ± 87 nM); solid squares $(cRGD)_2$ (IC_{50} of 66 ± 10 nM); solid triangles DOTA-$(cRGD)_2$ (IC_{50} of 316 ± 38 nM). All data represent mean ± SD (n = 3).

compared with cRGD monomer demonstrated the polyvalency effect typical of multimeric peptides. DOTA conjugation to $(cRGD)_2$ had a marginal impact on its binding affinity to integrin $\alpha_v\beta_3$.

PET/CT Imaging of Integrin $\alpha_v\beta_3$ Expression. The *in vivo* tumor homing capabilities of ^{44}Sc-DOTA-$(cRGD)_2$ were evaluated in nude mice bearing U87MG tumor xenografts (n = 3 per group) by multiple time-point static PET scans. Figure 3A shows representative coronal images of planes containing the tumor at 0.5, 2, and 4 h after intravenous injection of the tracer. Excellent tumor delineation was achieved owing to the observed exquisite tumor-to-background contrast. Quantitative ROI analysis was performed to quantify the tracer uptake values in the tumor and other major organs/tissues (Figure 3B and Table S1, Supporting Information). For all three time points, U87MG tumors showed a high persistent tracer uptake, which reached 3.93 ± 1.19, 3.07 ± 1.17, and 3.00 ± 1.25 %ID/g at 0.5, 2, and 4 h p.i., respectively (n = 3). A rapid renal clearance of ^{44}Sc-DOTA-$(cRGD)_2$ was evidenced by the low blood activities observed from early time points (0.98 ± 0.14 %ID/g at 0.5 h p.i.), the obvious kidney uptake (3.53 ± 1.36, 1.63 ± 0 0.47, and 1.50 ± 0.44 %ID/g at 0.5, 2, and 4 h p.i., respectively), and the presence of significant activities in the bladder (Figure 3B,D). Much lower nonspecific uptake in muscle and other nontarget tissues were recorded, providing increasingly high tumor-to-normal tissue (T/NT) ratios (Figure 3C).

The *in vivo* binding specificity of ^{44}Sc-DOTA-$(cRGD)_2$ for integrin $\alpha_v\beta_3$ was demonstrated through a receptor saturation/blocking experiment. A large excess of a blocking agent, 50 mg/kg (~1 mg) of $(cRGD)_2$ was coinjected with the tracer before sequential PET scans. As indicated in Figure 3A, coinjection of $(cRGD)_2$ resulted in a significant decline ($P < 0.05$) in tumor uptake values: 1.02 ± 0.25, 0.14 ± 0.04, and 0.06 ± 0.01 %ID/g at 0.5, 2, and 4 h p.i., respectively (n = 3; Figure 3E). Concomitantly, the tracer also showed a much faster renal clearance, which is typically observed for such blocking studies.

Biodistribution Studies. To validate PET data and obtain a more detailed distribution profile of ^{44}Sc-DOTA-$(cRGD)_2$, mice were euthanized immediately after the last PET scan at 4 h p.i., and *ex vivo* biodistribution studies were carried out. In agreement with PET imaging observations, a high accretion of the tracer in U87MG tumors (2.48 ± 0.76 %ID/g; n = 3) was observed (Figure 4). The normal tissues/organs presented markedly lower uptake compared to the tumor (Table S2, Supporting Information), except the organs that are responsible for tracer clearance (e.g., kidneys, liver, spleen, and intestine). In mice injected with a blocking dose of $(cRGD)_2$, tracer accumulation was significantly diminished in U87MG tumors. Interestingly, the uptake was also reduced in nontarget organs by the blocking dose, which indicated that the uptake of the tracer in these organs was partially mediated by the expression of integrin $\alpha_v\beta_3$. In fact, the expression of integrin $\alpha_v\beta_3$ in the vasculature of several of these tissues has been reported for rodents and humans.[14,33,34] Uptake in the kidneys was at a comparable level, 1.56 ± 0.48 vs 1.29 ± 0.26 %ID/g in nonblocked vs blocking groups, which ratified renal clearance as the main excretory pathway. Together these studies indicated excellent integrin $\alpha_v\beta_3$ specificity of the tracer *in vivo*.

DISCUSSION

PET-based molecular imaging is increasingly becoming a preferred means to scrutinize *in vivo* tumor biology in the clinic.[35] Within that niche, the evaluation of tumor angiogenesis stands out as one of the most extensively studied areas, for which RGD-based PET imaging plays a pivotal role.[35] The importance of this peptide family is underscored by the success attained in clinical trials using ^{18}F-labeled RGD analogues to image integrin $\alpha_v\beta_3$ in cancer patients.[21,22] However, ^{18}F-labeled radiopharmaceuticals may need significant improvements before widespread implementation in the clinic. Recent efforts suggested that radiolabeling with metallic isotopes may be preferable, with ^{64}Cu and ^{68}Ga as the alternatives. Nevertheless, the less common ^{44}Sc is now being recognized as a "better" isotope with the potential to improve several facets of current radiotracers, including radiosynthesis, quality of acquired images, dosimetry, and logistical aspects such as transportation of the agent to distant locations. Moreover, the existence of ^{47}Sc, a β^- emitter with suitable therapeutic properties, will warrant a place for ^{44}Sc in accurately determining dose distribution of analogous radiopharmaceuticals for cancer theranostics. On the basis of these promises, a few research groups including ours are investigating ^{44}Sc not only for peptide-based PET imaging but also for biomolecules with favorable pharmacokinetics (e.g., antibody fragment, affibodies, and small proteins).

Although the employment of isotopically enriched ^{44}Ca targets for cyclotron production of ^{44}Sc yield a product with radionuclidic purity surpassing 99%,[30] this method faces several practical hurdles. The poor performance of ^{44}Ca enriched materials (typically $^{44}CaCO_3$ or ^{44}CaO) as solid cyclotron targets (due to low electrical and heat conductivity), the necessity for target recycling, and most importantly, the highly fluctuating market of isotopically enriched isotopes, which could render ^{44}Sc production financially unviable, are some of the major reasons to seek other alternative production methods.[29] In a recently published work,[36] the irradiation of highly concentrated natural $Ca(NO_3)_2$ solutions for ^{44}Sc production was described. Despite the claimed advantages of this method, the low production yield inherent to the irradiation of liquid targets only allowed the productions of sub-mCi quantities of ^{44}Sc, which significantly limited the applicability of this method for large scale preclinical or clinical studies. Our production method, which improved upon our

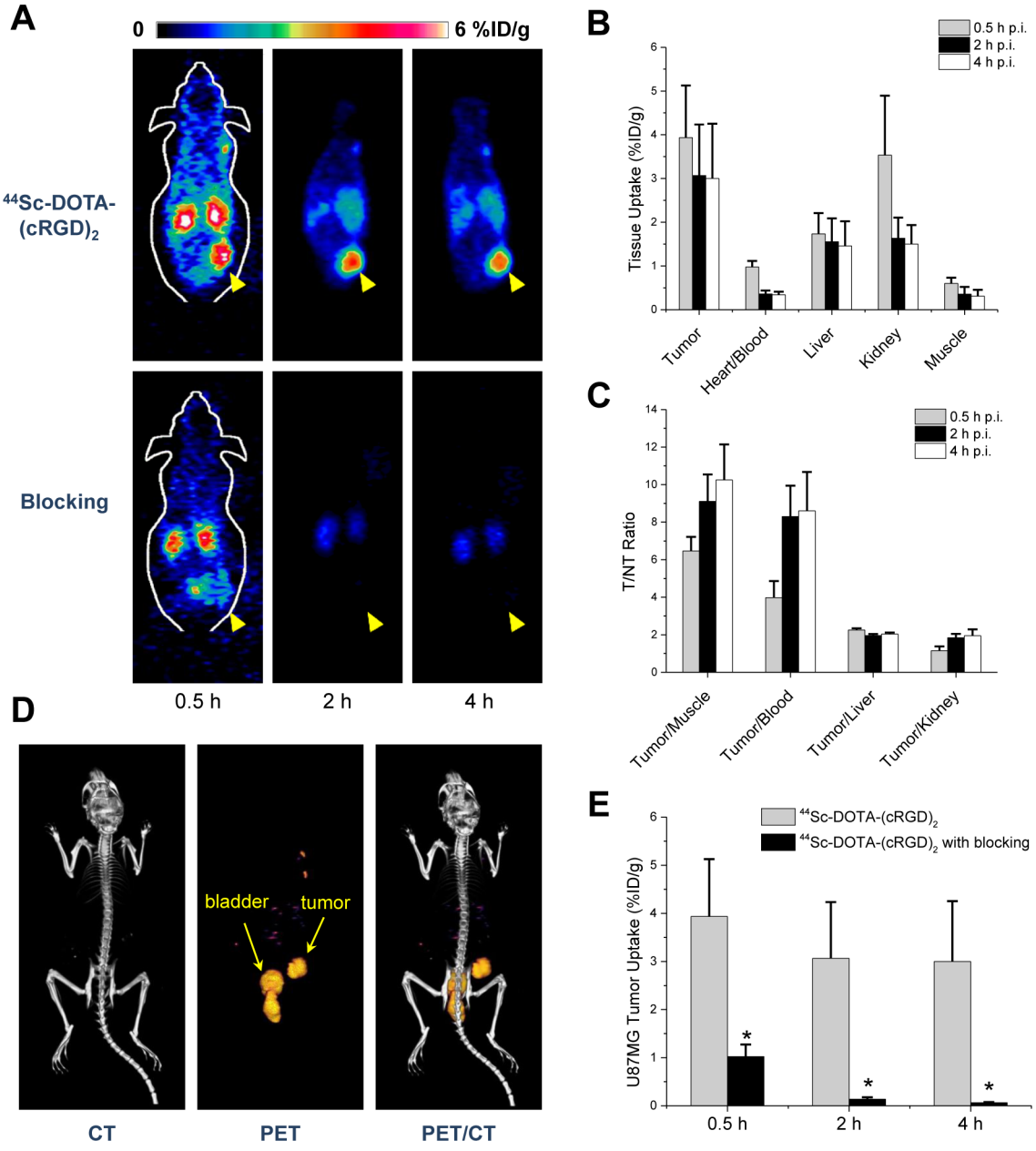

Figure 3. *In vivo* imaging studies with ^{44}Sc-DOTA-(cRGD)$_2$ in mice bearing U87MG xenografts. (A) Coronal images of sequential PET scans at 0.5, 2, and 4 h p.i. of either ^{44}Sc-DOTA-(cRGD)$_2$ (top row) or ^{44}Sc-DOTA-(cRGD)$_2$ with a blocking dose of (cRGD)$_2$ (50 mg/kg; bottom row); yellow arrowheads point to the tumor. (B) Tracer uptake (%ID/g) in U87MG tumors, blood pool, liver, kidneys, and muscle based on quantitative region-of-interest (ROI) analysis of the PET images. (C) Tumor-to-normal tissue (T/NT) ratios at 0.5, 2, and 4 h after injection. (D) Three-dimensional rendering of coregistered PET/CT images acquired 2 h after injection of the tracer, showing prominent uptake in the U87MG tumor and bladder. (E) Comparison of the tracer uptake in U87MG tumors between the nonblocking and blocking groups; * represents $P < 0.05$. $n = 3$.

previously reported method,[29] provides a simple and inexpensive mean to produce mCi levels of ^{44}Sc. The employment of natural Ca metal targets, with satisfactory solid target properties that include high electrical and thermal conductivities, a melting point over 1100 K, and low cost, provides the most cost-efficient production route for preclinical evaluation of ^{44}Sc-based radiopharmaceuticals. The principal disadvantage of this method is the decreased ^{44}Sc radionuclidic purities that irradiation of natural Ca provides. However, we determined that only two positron-emitting impurities ^{43}Sc and ^{44m}Sc were coproduced at a very low level (a few percent), which did not affect the quality of the PET imaging. In a clinical context, further evaluation of the dose associated with the presence of these impurities will be needed to evaluate the suitability of this production method for future translational investigation.

The separation of radioscandium by extraction chromatography using UTEVA resin was simple, fast, and efficient. Most of the produced activity (>90%) was trapped in the column, quantitatively eluted in ∼1 M HCl, and directly used for radiolabeling. Sc(III) is considered a pseudolanthanide, and its coordination chemistry closely resembles that of Y(III) and Lu(III). Chelation properties of Sc(III) have been well described for a myriad of chelating agents including several acyclic and macrocylic ligands (e.g., EDTA, DTPA, NOTA, and DOTA),[37] among which the DOTA complex features the best

dx.doi.org/10.1021/mp500343j | *Mol. Pharmaceutics* 2014, 11, 2954−2961

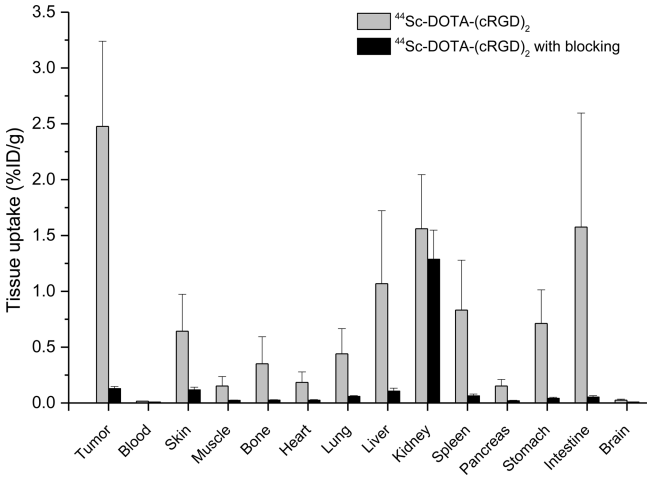

Figure 4. *Ex vivo* biodistribution of ^{44}Sc-DOTA-(cRGD)$_2$ and ^{44}Sc-DOTA-(cRGD)$_2$ coinjected with a blocking dose of (cRGD)$_2$ (50 mg/kg) in U87MG bearing mice at 4 h p.i. (n = 3).

thermodynamic stability (−log K = 27.0).[37] Owing to the excellent chelating properties of DOTA, we were able to successfully label DOTA-(cRGD)$_2$ with ^{44}Sc in high yields (>90%) and with a high specific activity of 7.4 GBq/μmol, which exceeded all previously reported values for Sc(III)-DOTA-peptide complexes.[27,30]

PET imaging with radiolabeled RGD peptides has been extensively studied over the past decade.[35,38] Numerous reports have employed positron-emitting radiometals such as ^{64}Cu and ^{68}Ga as the radiolabels.[4,6,14,18,39] However, ^{44}Sc, which possesses desirable properties for PET (e.g., high positron branching ratio, suitable decay $t_{1/2}$ that matches peptide pharmacokinetics, simple coordination chemistry, etc.), has been largely unexplored. In this study, we designed and characterized for the first time a ^{44}Sc-labeled RGD peptide for noninvasive PET imaging of tumor integrin $\alpha_v\beta_3$ expression in a human glioblastoma xenograft model. A dimeric cyclic RGD peptide, (cRGD)$_2$, was selected as the targeting moiety based on the enhanced affinity that multimeric peptides display for their targets.[6] The *in vitro* and *in vivo* binding affinity and specificity of ^{44}Sc-DOTA-(cRGD)$_2$ for integrin $\alpha_v\beta_3$ was investigated in detail via various experiments such as competitive cell-binding assay, blocking studies, PET scanning, and biodistribution studies. Taken together, these findings demonstrated that our results are comparable to previous reports on the use of ^{64}Cu-DOTA-(cRGD)$_2$ and ^{68}Ga-NOTA-(cRGD)$_2$ in the U87MG tumor model,[4,39] which further confirmed the broad potential of ^{44}Sc as a radionuclide of choice for peptide-based PET studies.

CONCLUSIONS

In this study, we established the feasibility of low-cost cyclotron produced ^{44}Sc, using natural Ca metal targets, and subsequent labeling of a dimeric RGD peptide for noninvasive PET imaging applications in a well-established U87MG xenograft model, which has a high level of integrin $\alpha_v\beta_3$ expression on both the tumor cells and tumor neovasculature. ^{44}Sc-DOTA-(cRGD)$_2$ was found to be comparable to other ^{64}Cu- and ^{68}Ga-labeled radiopharmaceuticals in terms of tumor targeting efficacy, pharmacokinetic profile, PET image quality, etc., which demonstrated the enormous potential of ^{44}Sc to become the radionuclide of choice for future PET procedures. The simple production, separation, and radiosynthesis methods reported in this work will facilitate future expansion of ^{44}Sc-based PET imaging applications. Improved radiolabeling strategies under mild conditions for the synthesis of heat-sensitive biomolecules (e.g., proteins and antibody fragments) are currently being explored.

ASSOCIATED CONTENT

Supporting Information

γ-Spectrum at EoB, HPLC profile of DOTA-(cRGD)$_2$, optimization of radiolabeling conditions, ROI analysis of PET scans, and biodistribution results. This material is available free of charge via the Internet at http://pubs.acs.org.

AUTHOR INFORMATION

Corresponding Author

*(W.C.) Fax: 1-608-265-0614. Phone: 1-608-262-1749. E-mail: wcai@uwhealth.org.

Notes

The authors declare no competing financial interest.

ACKNOWLEDGMENTS

The authors thank Dr. Feng Chen for his insightful comments on the manuscript and Justin Jeffery for his assistance with PET/CT imaging and scanner calibration. This work was supported, in part, by the University of Wisconsin−Madison, the Department of Defense (W81XWH-11-1-0644), the National Science Foundation (DGE-1256259), the National Institutes of Health (NIBIB/NCI 1R01CA169365, P30CA014520, and 5T32GM08349), the US Department of States sponsored Fulbright Scholar Program (1831/FNPDR/2013), and the American Cancer Society (125246-RSG-13-099-01-CCE).

REFERENCES

(1) Allen, E.; Walters, I. B.; Hanahan, D. Brivanib, a dual FGF/VEGF inhibitor, is active both first and second line against mouse pancreatic neuroendocrine tumors developing adaptive/evasive resistance to VEGF inhibition. *Clin. Cancer Res.* **2011**, *17*, 5299−310.

(2) Folkman, J. Seminars in Medicine of the Beth Israel Hospital, Boston. Clinical applications of research on angiogenesis. *N. Engl. J. Med.* **1995**, *333*, 1757−63.

(3) Ferrara, N. Vascular endothelial growth factor and the regulation of angiogenesis. *Recent Prog. Horm. Res.* **2000**, *55*, 15−35 discussion 35−6..

(4) Liu, Z.; Niu, G.; Shi, J.; Liu, S.; Wang, F.; Liu, S.; Chen, X. ^{68}Ga-labeled cyclic RGD dimers with Gly3 and PEG4 linkers: promising agents for tumor integrin alphavbeta3 PET imaging. *Eur. J. Nucl. Med. Mol. Imaging* **2009**, *36*, 947−57.

(5) Hanahan, D.; Folkman, J. Patterns and emerging mechanisms of the angiogenic switch during tumorigenesis. *Cell* **1996**, *86*, 353−64.

(6) Li, Z. B.; Cai, W.; Cao, Q.; Chen, K.; Wu, Z.; He, L.; Chen, X. (64)Cu-labeled tetrameric and octameric RGD peptides for small-animal PET of tumor alpha(v)beta(3) integrin expression. *J. Nucl. Med.* **2007**, *48*, 1162−71.

(7) Puduvalli, V. K. Inhibition of angiogenesis as a therapeutic strategy against brain tumors. *Cancer Treat. Res.* **2004**, *117*, 307−36.

(8) Sengupta, S.; Chattopadhyay, N.; Mitra, A.; Ray, S.; Dasgupta, S.; Chatterjee, A. Role of alphavbeta3 integrin receptors in breast tumor. *J. Exp. Clin. Cancer Res.* **2001**, *20*, 585−90.

(9) Felding-Habermann, B.; Fransvea, E.; O'Toole, T. E.; Manzuk, L.; Faha, B.; Hensler, M. Involvement of tumor cell integrin alphavbeta3 in hematogenous metastasis of human melanoma cells. *Clin. Exp. Metastasis* **2002**, *19*, 427−36.

(10) Bello, L.; Francolini, M.; Marthyn, P.; Zhang, J.; Carroll, R. S.; Nikas, D. C.; Strasser, J. F.; Villani, R.; Cheresh, D. A.; Black, P. M. Alphavbeta3 and alphavbeta5 integrin expression in glioma periphery. *Neurosurgery* **2001**, *49*, 380−9 discussion 390..
(11) Jin, H.; Varner, J. Integrins: roles in cancer development and as treatment targets. *Br. J. Cancer* **2004**, *90*, 561−5.
(12) Kumar, C. C. Integrin alphavbeta3 as a therapeutic target for blocking tumor-induced angiogenesis. *Curr. Drug Targets* **2003**, *4*, 123−31.
(13) Kumar, C. C.; Armstrong, L.; Yin, Z.; Malkowski, M.; Maxwell, E.; Ling, H.; Yaremko, B.; Liu, M.; Varner, J.; Smith, E. M.; Neustadt, B.; Nechuta, T. Targeting integrins alpha v beta 3 and alphavbeta5 for blocking tumor-induced angiogenesis. *Adv. Exp. Med. Biol.* **2000**, *476*, 169−80.
(14) Dijkgraaf, I.; Yim, C. B.; Franssen, G. M.; Schuit, R. C.; Luurtsema, G.; Liu, S.; Oyen, W. J.; Boerman, O. C. PET imaging of alphavbeta3 integrin expression in tumours with ^{68}Ga-labelled mono-, di- and tetrameric RGD peptides. *Eur. J. Nucl. Med. Mol. Imaging* **2011**, *38*, 128−37.
(15) Cai, W.; Wu, Y.; Chen, K.; Cao, Q.; Tice, D. A.; Chen, X. In vitro and in vivo characterization of 64Cu-labeled Abegrin, a humanized monoclonal antibody against integrin alphavbeta3. *Cancer Res.* **2006**, *66*, 9673−81.
(16) Plow, E. F.; Haas, T. A.; Zhang, L.; Loftus, J.; Smith, J. W. Ligand binding to integrins. *J. Biol. Chem.* **2000**, *275*, 21785−8.
(17) Terry, S. Y.; Abiraj, K.; Frielink, C.; van Dijk, L. K.; Bussink, J.; Oyen, W. J.; Boerman, O. C. Imaging integrin alphavbeta3 on blood vessels with 111In-RGD2 in head and neck tumor xenografts. *J. Nucl. Med.* **2014**, *55*, 281−6.
(18) Trajkovic-Arsic, M.; Mohajerani, P.; Sarantopoulos, A.; Kalideris, E.; Steiger, K.; Esposito, I.; Ma, X.; Themelis, G.; Burton, N.; Michalski, C. W.; Kleeff, J.; Stangl, S.; Beer, A. J.; Pohle, K.; Wester, H. J.; Schmid, R. M.; Braren, R.; Ntziachristos, V.; Siveke, J. T. Multimodal molecular imaging of integrin alphavbeta3 for in vivo detection of pancreatic cancer. *J. Nucl. Med.* **2014**, *55*, 446−51.
(19) Haubner, R.; Wester, H. J.; Burkhart, F.; Senekowitsch-Schmidtke, R.; Weber, W.; Goodman, S. L.; Kessler, H.; Schwaiger, M. Glycosylated RGD-containing peptides: tracer for tumor targeting and angiogenesis imaging with improved biokinetics. *J. Nucl. Med.* **2001**, *42*, 326−36.
(20) Haubner, R.; Wester, H. J.; Weber, W. A.; Mang, C.; Ziegler, S. I.; Goodman, S. L.; Senekowitsch-Schmidtke, R.; Kessler, H.; Schwaiger, M. Noninvasive imaging of alpha(v)beta3 integrin expression using 18F-labeled RGD-containing glycopeptide and positron emission tomography. *Cancer Res.* **2001**, *61*, 1781−5.
(21) Beer, A. J.; Haubner, R.; Sarbia, M.; Goebel, M.; Luderschmidt, S.; Grosu, A. L.; Schnell, O.; Niemeyer, M.; Kessler, H.; Wester, H. J.; Weber, W. A.; Schwaiger, M. Positron emission tomography using [18F]Galacto-RGD identifies the level of integrin alpha(v)beta3 expression in man. *Clin. Cancer Res.* **2006**, *12*, 3942−9.
(22) Kenny, L. M.; Coombes, R. C.; Oulie, I.; Contractor, K. B.; Miller, M.; Spinks, T. J.; McParland, B.; Cohen, P. S.; Hui, A. M.; Palmieri, C.; Osman, S.; Glaser, M.; Turton, D.; Al-Nahhas, A.; Aboagye, E. O. Phase I trial of the positron-emitting Arg-Gly-Asp (RGD) peptide radioligand 18F-AH111585 in breast cancer patients. *J. Nucl. Med.* **2008**, *49*, 879−86.
(23) Breeman, W. A.; de Blois, E.; Sze Chan, H.; Konijnenberg, M.; Kwekkeboom, D. J.; Krenning, E. P. (68)Ga-labeled DOTA-peptides and (68)Ga-labeled radiopharmaceuticals for positron emission tomography: current status of research, clinical applications, and future perspectives. *Semin. Nucl. Med.* **2011**, *41*, 314−21.
(24) Roesch, F.; Riss, P. J. The renaissance of the ^{68}Ge/^{68}Ga radionuclide generator initiates new developments in ^{68}Ga radiopharmaceutical chemistry. *Curr. Top. Med. Chem.* **2010**, *10*, 1633−68.
(25) Anderson, C. J.; Ferdani, R. Copper-64 radiopharmaceuticals for PET imaging of cancer: Advances in preclinical and clinical research. *Cancer Biother. Radiopharm.* **2009**, *24*, 379−393.
(26) Kolsky, K. L.; Joshi, V.; Mausner, L. F.; Srivastava, S. C. Radiochemical purification of no-carrier-added scandium-47 for radioimmunotherapy. *Appl. Radiat. Isot.* **1998**, *49*, 1541−9.
(27) Koumarianou, E.; Loktionova, N. S.; Fellner, M.; Roesch, F.; Thews, O.; Pawlak, D.; Archimandritis, S. C.; Mikolajczak, R. ^{44}Sc-DOTA-BN[2−14]NH2 in comparison to ^{68}Ga-DOTA-BN[2−14]NH2 in pre-clinical investigation. Is ^{44}Sc a potential radionuclide for PET? *Appl. Radiat. Isot.* **2012**, *70*, 2669−76.
(28) Filosofov, D. V.; Loktionova, N. S.; Roesch, F. A ^{44}Ti/^{44}Sc radionuclide generator for potential nuclear-medical application of ^{44}Sc-based PET-radiopharmaceuticals. *Radiochim. Acta* **2010**, *98*, 149−156.
(29) Severin, G. W.; Engle, J. W.; Valdovinos, H. F.; Barnhart, T. E.; Nickles, R. J. Cyclotron produced ^{44g}Sc from natural calcium. *Appl. Radiat. Isot.* **2012**, *70*, 1526−30.
(30) Muller, C.; Bunka, M.; Reber, J.; Fischer, C.; Zhernosekov, K.; Turler, A.; Schibli, R. Promises of cyclotron-produced 44Sc as a diagnostic match for trivalent beta−emitters: in vitro and in vivo study of a 44Sc-DOTA-folate conjugate. *J. Nucl. Med.* **2013**, *54*, 2168−74.
(31) Wu, Y.; Zhang, X.; Xiong, Z.; Cheng, Z.; Fisher, D. R.; Liu, S.; Gambhir, S. S.; Chen, X. microPET imaging of glioma integrin alphavbeta3 expression using (64)Cu-labeled tetrameric RGD peptide. *J. Nucl. Med.* **2005**, *46*, 1707−18.
(32) Valdovinos, H. F.; Hernandez, R.; Barnhart, T. E.; Cai, W.; Nickles, R. J. Unpublished work. University of Wisconsin, Madison, WI, 2014.
(33) Max, R.; Gerritsen, R. R.; Nooijen, P. T.; Goodman, S. L.; Sutter, A.; Keilholz, U.; Ruiter, D. J.; De Waal, R. M. Immunohistochemical analysis of integrin alphavbeta3 expression on tumor-associated vessels of human carcinomas. *Int. J. Cancer.* **1997**, *71*, 320−4.
(34) Wu, Z.; Li, Z. B.; Chen, K.; Cai, W.; He, L.; Chin, F. T.; Li, F.; Chen, X. microPET of tumor integrin alphavbeta3 expression using 18F-labeled PEGylated tetrameric RGD peptide (18F-FPRGD4). *J. Nucl. Med.* **2007**, *48*, 1536−44.
(35) Cai, W.; Niu, G.; Chen, X. Imaging of integrins as biomarkers for tumor angiogenesis. *Curr. Pharm. Des.* **2008**, *14*, 2943−73.
(36) Hoehr, C.; Oehlke, E.; Benard, F.; Lee, C. J.; Hou, X.; Badesso, B.; Ferguson, S.; Miao, Q.; Yang, H.; Buckley, K.; Hanemaayer, V.; Zeisler, S.; Ruth, T.; Celler, A.; Schaffer, P. ^{44g}Sc production using a water target on a 13MeV cyclotron. *Nucl. Med. Biol.* **2014**, *41*, 401−6.
(37) Majkowska-Pilip, A.; Bilewicz, A. Macrocyclic complexes of scandium radionuclides as precursors for diagnostic and therapeutic radiopharmaceuticals. *J. Inorg. Biochem.* **2011**, *105*, 313−20.
(38) Cai, W.; Chen, X. Multimodality molecular imaging of tumor angiogenesis. *J. Nucl. Med.* **2008**, *49* (Suppl2), 113S−28S.
(39) Shi, J.; Kim, Y. S.; Zhai, S.; Liu, Z.; Chen, X.; Liu, S. Improving tumor uptake and pharmacokinetics of (64)Cu-labeled cyclic RGD peptide dimers with Gly(3) and PEG(4) linkers. *Bioconjugate Chem.* **2009**, *20*, 750−9.